Archives of Razi Institute Journal
"Arch. Razi Inst."

Journal Homepage: https://archrazi.areeo.ac.ir/

Research Paper

Androctonus Nazarii, a New Species of Scorpions From Khuzestan Province, Iran (Scorpiones: Buthidae)

Fatemeh Salabi[1*], Bahman Zangi[2], Alireza Forouzan[1], Mohammad Hossein Jahan-Mahin[2], Seyed Mahdi Kazemi[2]

1. Department of Venomous Animals and Anti-Venom Production, Razi Vaccine and Serum Research Institute, Agricultural Research, Education and Extension Organization (AREEO), Ahvaz, Iran.
2. Zagros Herpetological Institute, Qom, Iran.

Use your device to scan and read the article online

How to cite this article Salabi F, Zangi B, Forouzan A, Jahan-Mahin MH, Kazemi SM. *Androctonus Nazarii*, a New Species of Scorpions From Khuzestan Province, Iran (Scorpiones: Buthidae). Archives of Razi Institute Journal. 2025; 80(6):1567-1580. https://doi.org/10.32598/ARI.80.6.3928

https://doi.org/10.32598/ARI.80.6.3928

Article info:
Received: 01 Aug 2025
Accepted: 25 Aug 2025
Published: 01 Nov 2025

Keywords:
Androctonus nazarii, Khuzestan Province, Morphological features, New species, Zagros Mountains

ABSTRACT

Introduction: Recent research has clarified the historically complex taxonomy of the medically significant scorpion genus *Androctonus* in Iran, chiefly by resolving the *A. crassicauda* Olivier, 1807 species complex and describing numerous new species. However, the taxonomic status of certain populations in Khuzestan Province (south-western Iran) has remained unsettled.

Materials & Methods: The new scorpion species, *Androctonus nazarii* sp. nov., was collected from Baghmalek in the Zagros Mountains of Khuzestan Province, Iran. The species description is based on two male specimens, which were characterized by a set of distinct morphological features.

Results: The species exhibits distinctive diagnostic characteristics, including a brownish-yellow coloration, a light brown carapace devoid of ocular black patches and featuring fine granulation, uniformly yellow legs, and a specific yellowish-brown, finely granulated chela manus. A detailed comparison with its closest relatives (*A. crassicauda*, *A. zagrosensis*, *A. sumericus*, and *A. barahoeii*) confirms its distinctiveness.

Conclusion: Its discovery fills an important taxonomic gap in south-western Iran and carries significant implications for public health and conservation.

*** Corresponding Author:**
Fatemeh Salabi, Assistant Professor.
Address: *Department of Venomous Animals and Anti-Venom Production, Razi Vaccine and Serum Research Institute, Agricultural Research, Education and Extension Organization (AREEO), Ahvaz, Iran.*
Tel: *+98 (61) 33334503*
E-mail: *f.salabi@rvsri.ac.ir*

1. Introduction

Iran harbors a remarkably diverse scorpion fauna, dominated by the family Buthidae [1-4]. This richness is fostered by the country's complex topography and diverse climates, which have given rise to 18 recognized terrestrial ecoregions [5-8]. The documented fauna includes 99 species from 20 genera, with a high rate of endemism (74 species). Within this fauna, the genus *Androctonus Ehrenberg*, 1828 is of critical medical importance due to the potent venom of its species, representing a significant public health concern [9, 10]. The taxonomy of *Androctonus* has long been challenging due to pronounced morphological convergence and high intraspecific variation [11, 12]. This challenge was exemplified in Iran, where for decades diverse populations were broadly classified under a single species, *A. crassicauda* [13, 1, 14]. Recent integrative taxonomic studies have revolutionized this understanding, revealing that these populations represent a complex of distinct species. This paradigm shift has prompted the description of numerous new *Androctonus* species throughout the Middle East. Notable examples from the region now include *A. turkiyensis* and *A. kunti* in Turkey, respectively [15]; *A. ammoneus* in Jordan [16]; *A. omanensis* and *A. ammophilus* in Oman [17]; *A. sumericus* (Dhi Qar Province) and *A. ishtar* (Duhok and Nineveh Provinces) in Iraq [18, 16]; *A. tihamicus* in Saudi Arabia [19]; and several from Iran, such as *A. sistanus*, *A. orientalis*, and *A. zagrosensis* [20, 15, 10] from Iran. A comprehensive review by Yağmur et al. [15] further resolved the taxonomy of *Prionurus crassicauda orientalis* Birula, 1900, elevating it to species rank as *A. rostami*. Consequently, the genus now includes 49 species, with nine currently recognized from Iran include: *A. crassicauda* (Olivier, 1807); *A. orientalis* (Birula, 1900); *A. sistanus* Barahoei and Mirshamsi, 2022; *A. sumericus* Al-Khazali and Yağmur, 2023; *A. transcaucasisus* Kovařík, Yağmur, Fet and Lowe, 2025; *A. azerianus* Yağmur and Kovařík 2025; *A. caspius* Kovařík, Yağmur, Fet and Lowe, 2025; *A. barahoeii* Kovařík and Yağmur, 2025, and *A. zagrosensis* Kazemi and Salabi, 2025 [13, 15, 18, 20-22]. According to Kazemi et al., the genus *Androctonus* is one of two deadly genus scorpions of Iran [23]. Despite these significant advances, the taxonomic status of *Androctonus* populations in several Iranian provinces, including Khuzestan, has remained unclear. Khuzestan Province, located in southwestern Iran, is a critical area of study. It encompasses four distinct ecoregions—the South Iran Nubo-Sindian desert and semi-desert, the Tigris-Euphrates alluvial salt marsh, the Zagros Mountains forest steppe, and the Arabian Desert and East Saharo-Arabian xeric shrublands—whose ecological convergence supports an exceptionally rich scorpion fauna. The province is home to over 30 species, representing approximately one-third of Iran's total diversity [8, 24]. Although recent work has begun to clarify its diversity, with species such as *A. zagrosensis*, *A. barahoeii*, and *A. sumericus* being described from the province, significant gaps in our understanding persist. Here, we describe a previously unreported species, *A. nazarii* sp. nov., from Baghmalek, Khuzestan, whose medical importance was previously unassessed. We investigate this population by comparing it morphologically with its closest relatives, including *A. crassicauda*, *A. zagrosensis*, *A. sumericus*, and *A. barahoeii*.

2. Material and Methods

2.1. Specimen collection

Approximately 50 specimens of *Androctonus* sp. were collected at night using ultraviolet light detection in Baghmalek, Khuzestan Province, Iran, in August 2025 (Figures 1 and 2). Based on distinct morphological coloration, two individuals were selected and preserved in 96% ethanol for morphological analyses. Voucher specimens, including the holotype (mature male) and paratype (immature male) of *A. nazarii* sp. nov., have been deposited in the Venomous Animals Museum of the Razi Vaccine and Serum Research Institute, Karaj, Alborz, Iran.

2.2. Morphological analysis

Morphological examination was conducted on two males (one mature, one immature) using a Leica MZ 7.5 stereomicroscope. The assessment followed the taxonomic frameworks of Sissom et al. [25] and Yağmur [26], with a focus on coloration, pedipalp morphology, and prosomal/metasomal features. Standardized imaging was performed according to the protocol of Yağmur [26]. Morphometric data, comprising six meristic traits and 18 morphometric ratios, were recorded in millimeters (mm) using digital calipers.

2.3. Abbreviations of morphometric ratios

CL: Carapace length; CPW: Carapace posterior wide; CAW: Carapace anterior wide; CHL: Manus+ fixed finger length; ML: Manus length; MFL: Movable finger length; No.MFT: Number of Movable fig teeth (L: Left; R: Right); No.FFT: Number of fixed finger teeth (L: Left; R: Right); No.PT: Number of pectinal teeth (L:

Left; R: Right); Body length: BL; Mt(I-V)L: Metasomal segment I-V length; Mt(I-V)W: Metasomal segment I-V wide; RVSRI; Razi Vaccine and Serum Research Institute; VAMRVSRI: Venomous Animals Museum of Razi Vaccine and Serum Research Institute, Karaj, Alborz, Iran.

3. Results

3.1. Systematic description

Order Scorpiones C.L. Koch, 1837

Family Buthidae C.L. Koch, 1837

Genus *Androctonus Ehrenberg*, 1828

A. nazarii sp. nov. (Figures 2, 3, 4, 5, 6, 7, 8, 9, and 10)

Material examined (2 specimens including 2 males)

Holotype: 1♂ (VAMRVSRI, catalog number VAMRVSRI-SA010), Iran, Khuzestan Province, Baghmalek, Qaleh tol, 10 km NW of Qaleh tol, 31.618°N, 49.961°E, elev. 800 m, 15 September 2025, leg. F. Salabi. Paratypes: 1♂ (same locality as holotype, 15 September 2025, leg. F. Salabi leg.

3.2. Etymology

The species epithet is a patronym honoring Mahmood Nazari for his contributions to scorpion taxonomy and diversity in Khuzestan, Iran.

3.3. Type locality

Iran, Khuzestan Province, Baghmalek, Qaleh tol.

3.4. Geographical distribution

Populations of this species are distributed in the southwestern Iran, Baghmalek, Bakhmali region (Qaleh tol to AblashkareOlya).

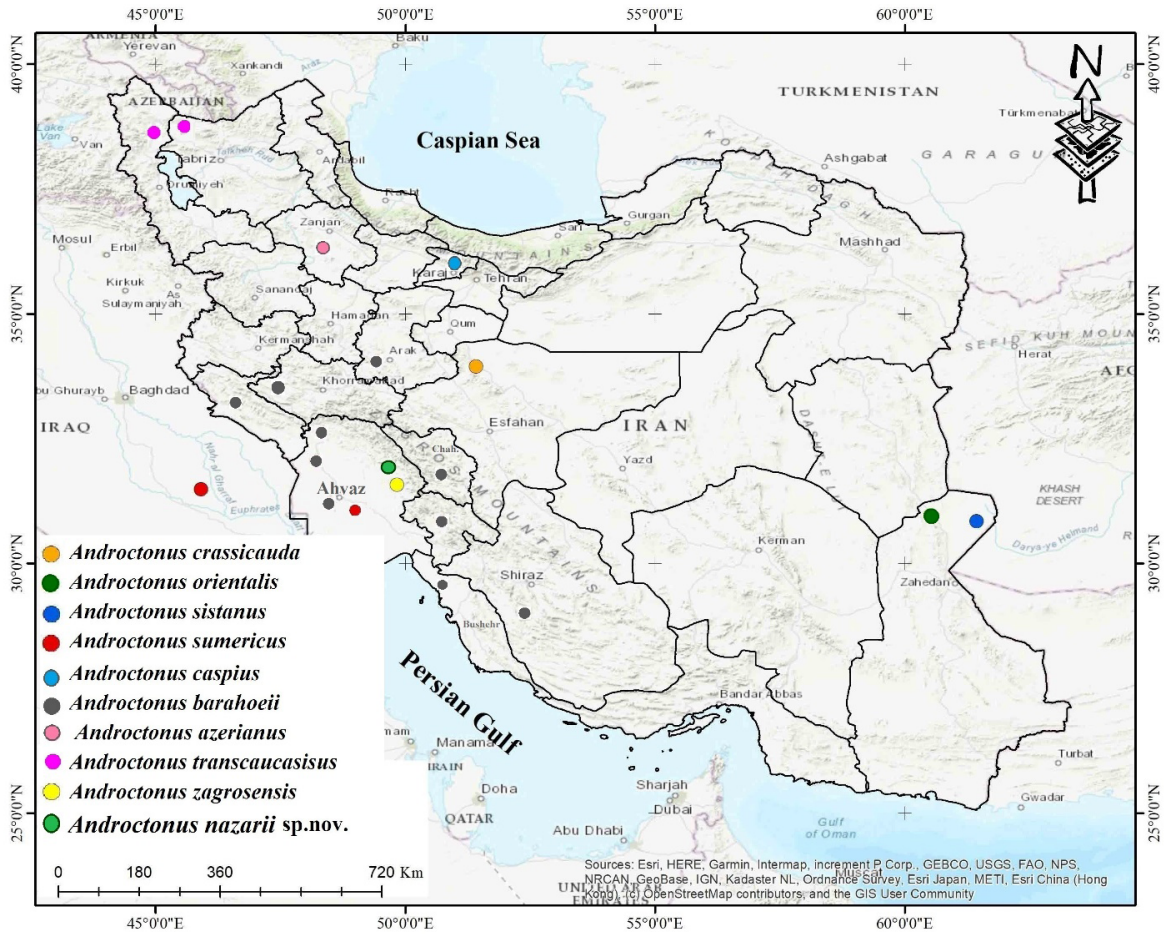

Figure 1. Localities of *Androctonus* genus in Iran and sampling area of *Androctonus nazarii* sp. nov. from Baghmalek, Khuzestan, Iran

Figure 2. Holotype specimen of *A. nazarii* sp. nov. from Baghmalek, Khuzestan, Iran

A) Dorsal view; B) Ventral view (scale bar: 10 mm)

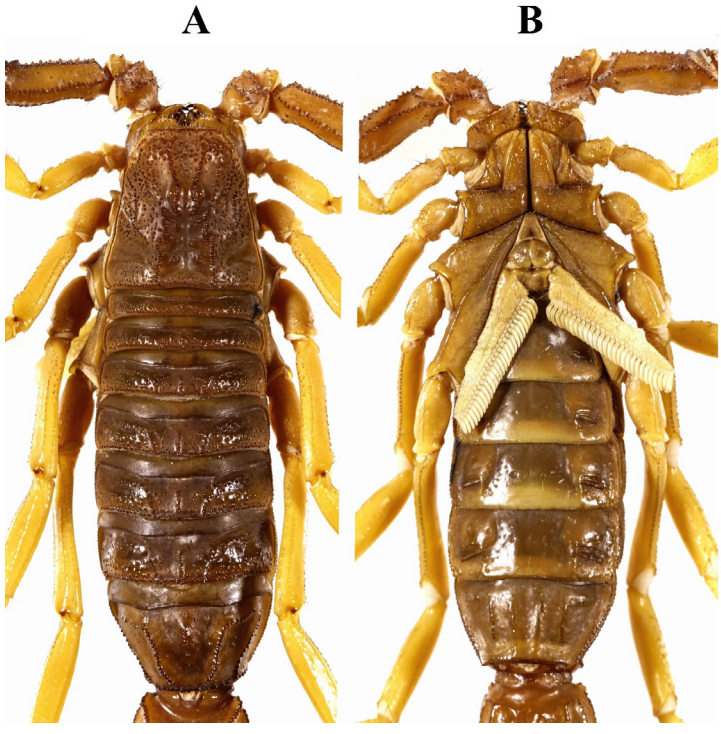

Figure 3. Holotype specimen of *A. nazarii* sp. nov. from Baghmalek, Khuzestan, Iran

A) Carapace and mesosoma; B) Sternopectinal area and ventral of mesosoma

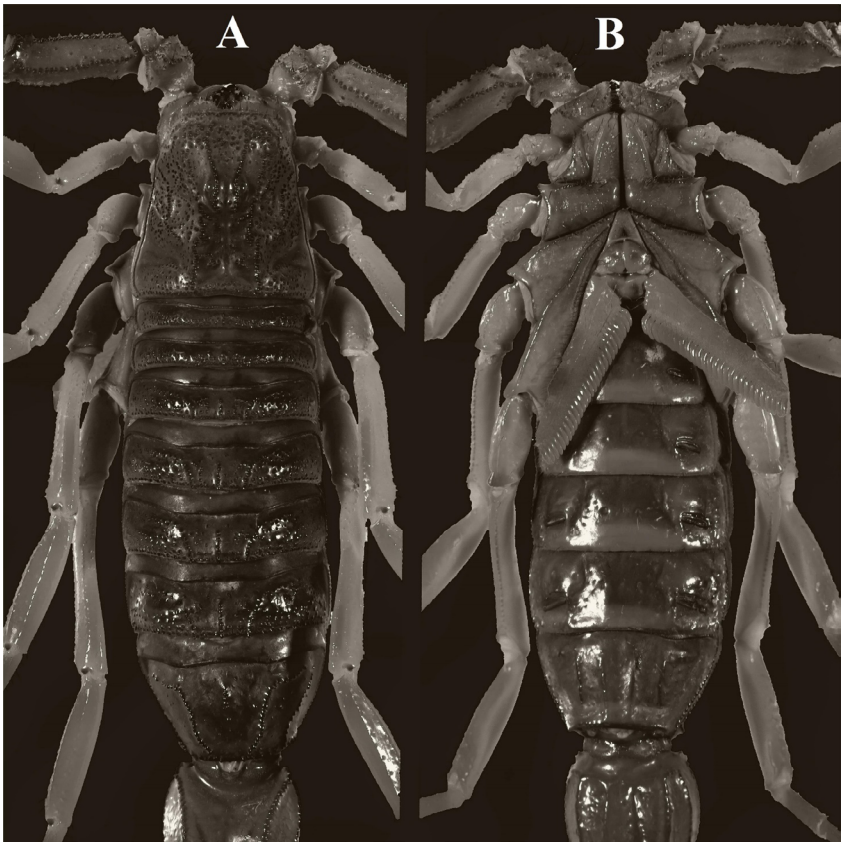

Figure 4. Holotype specimen of *A. nazarii* sp. nov. from Baghmalek, Khuzestan, Iran

A) Carapace and mesosoma; B) Sternopectinal area and ventral of mesosoma

Figure 5. Holotype specimen of *A. nazarii* sp. nov. from Baghmalek, Khuzestan, Iran (carapace and sternopectinal area)

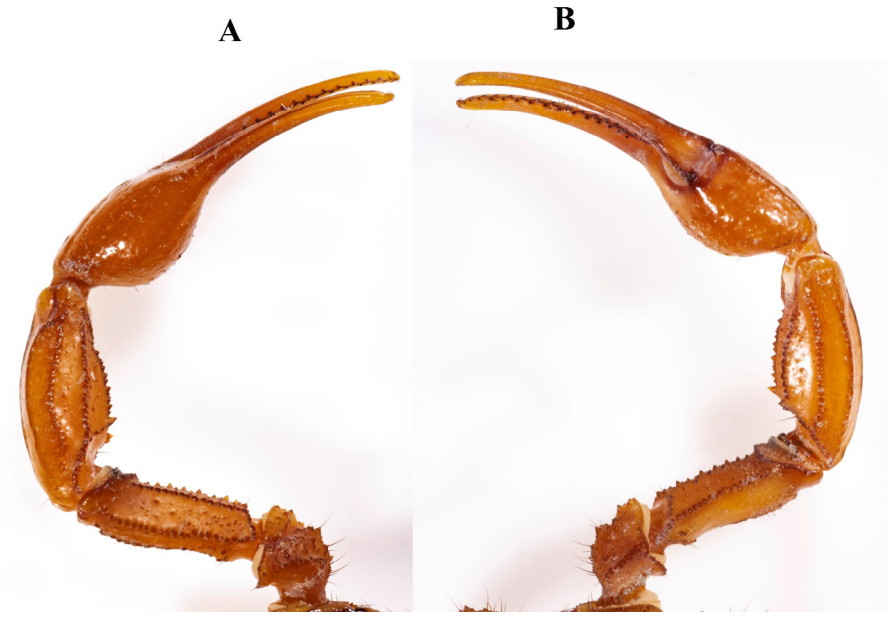

Figure 6. Holotype specimen of *A. nazarii* sp. nov. from Baghmalek, Khuzestan, Iran

A) Dorsal view of pedipalp; B) Ventral view of pedipalp

3.5. Diagnosis (1♂ holotype)

A. nazarii sp. nov. is a medium-sized species (adult body length 66.88 mm). The base color light brown to brownish-yellow; the ocular area surrounding the median eyes and the lateral eyes lacks a distinctive black patch; pedipalps, metasomal segments I–V and telson brownish-yellow; legs uniformly yellow, without any spots in males. A unique feature of this scorpion is the high-contrast black carinae found on parts of its carapace, pedipalps, and metasoma. The pectinal tooth count

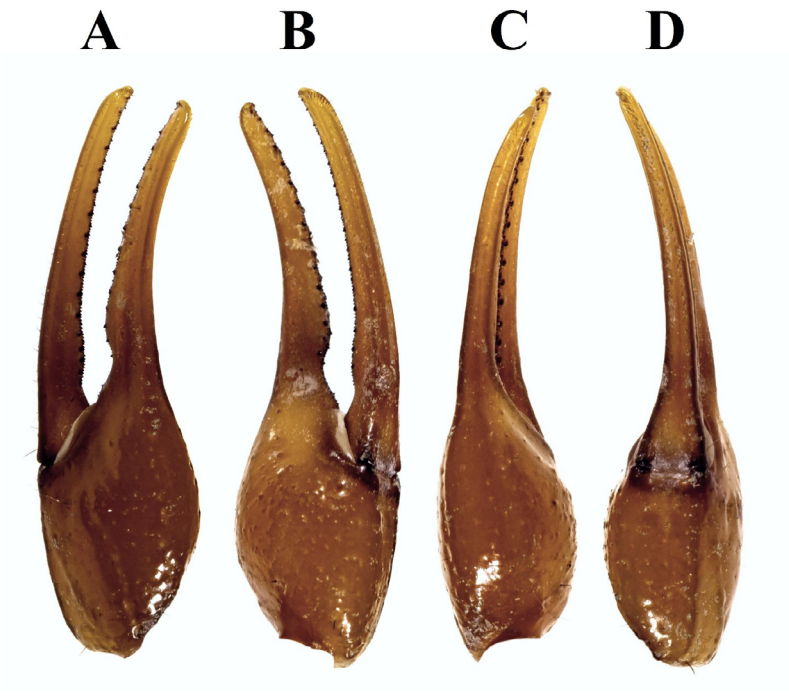

Figure 7. Holotype specimen of *A. nazarii* sp. nov. from Baghmalek, Khuzestan, Iran

A) External view of chela; B) Internal view of chela; C) Dorsal view of chela; D) Ventral view of chela

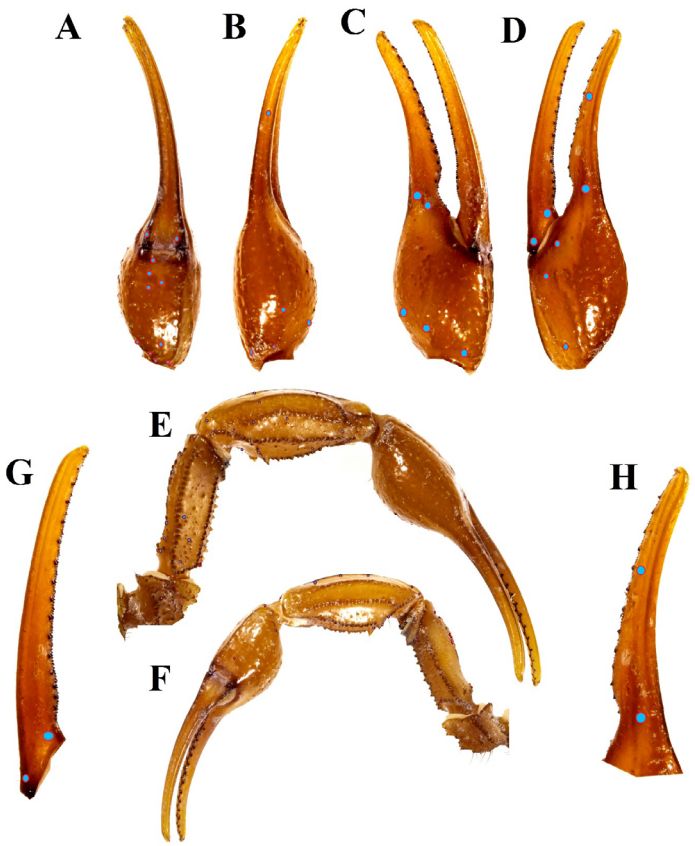

Figure 8. Holotype specimen of *A. nazarii* sp. nov. from Baghmalek, Khuzestan, Iran

A) Ventral view of chela; B) Dorsal view of chela; C) Internal view of chela; D) External view of chela; E) Dorsal view of pedipalps; F) Ventral view of pedipalps; G) Movable finger dentition; H) Fixed finger dentition

Note: Trichobothrial pattern is indicated by blue circles.

27–28. The carapace exhibits dense, fine granulation, lacking large granules. The pedipalps are stocky.

Femur. Pentacarinate; all carinae well-developed and granular; intercarinal surfaces with scattered granules; the external surface becoming mostly smooth posteriorly.

Patella. Octocarinate; dorsal, ventral, and external surfaces smooth or with very few scattered granules; internal surface finely granulated; dorsal prolateral and ventral prolateral carinae strongly crenulated, bearing coarse, pointed, conical granules, each demarcated anteriorly by a large macroseta and associated with a well-developed patellar spur; dorsal retrolateral and ventral retrolateral carinae weak to obsolete. The fixed and movable fingers possess 14–15 and 15–16 principal rows of denticles, respectively.

Sternite. Sternites I-VII are uniformly light brown with dull yellow posterior margins; sternites I-VI are smooth and lack carinae, while sternite VII possesses four carinae on an otherwise smooth surface.

Metasoma. Measoma I–V are smooth dorsally and laterally, granulate ventrally; segments I–V possess 10-8-8-8-5 carinae, respectively; the lateral inframedian carinae are complete on segment I, reduced to 4 coarse granules on II and 3 granules on III, and absent on IV–V. The fifth metasomal segment possesses moderately developed ventrolateral carinae, which bear granules that gradually and slightly increase in size posteriorly, culminating in four enlarged, rounded, and widely spaced granules. The dorsal carinae of segments I–IV and dorsolateral carinae of segments I–III are strong, bearing large, serrate granules that gradually increase in size posteriorly and end in two large posterior granules. The dorsolateral carinae of segment V have large, distinct, rounded anterior granules and no posterior granules.

Telson. Elongated; dorsally smooth with a pair of large symmetrical granules, ventrally granulate and ridged (Figures 2, 3, 4, 5, 6, 7, 8, 9, and 10).

Archives of Razi Institute Journal

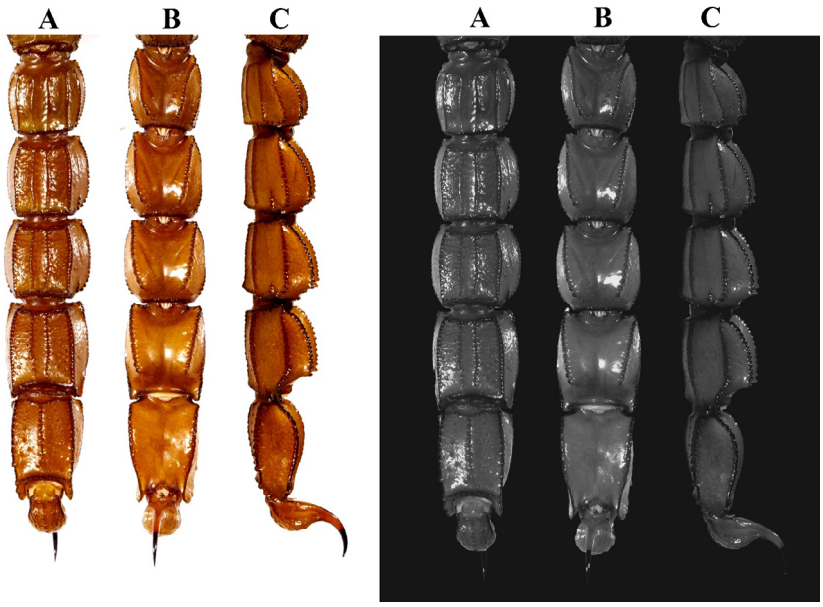

Figure 9. Holotype specimen of *A. nazarii* sp. nov. from Baghmalek, Khuzestan, Iran

Note: Metasoma and telson of adult male holotype: A) Ventral view; B) Dorsal view; C) Lateral view.

Figure 10. Holotype specimen of *A. nazarii* sp. nov. from Baghmalek, Khuzestan, Iran: Right legs I–IV

3.6. Description

(♂♀): Description is based on the 1♂ holotype (VAM-RVSRI-AZ010) and the ♂ paratype.

3.7. Coloration

The body (from prosoma to telson) display differing pigmentation, ranging from brown to yellowish-brown and yellow (Figures 2 and 3).

Carapace. Predominantly brown, grading from a light anterior to a dark posterior; its carinae and granules are a darker shade, ranging from brown to blackish-brown. In males, the ocular area surrounding the median eyes lacks a distinctive black patch and the ocular area surrounding the lateral eyes lacks a color patch (Figures 3 and 4); the median eyes themselves are uniformly light brown (Figures 3 and 5).

Chelicerae. Manus is yellowish-brown; fingers yellowish-brown, with blackish-brown teeth.

Pedipalps. The femur and patella are brownish-yellow on both the dorsal and ventral surfaces; their internal and external carinae are dark brown and feature brown median carinae and granules dorsally and ventrally (Figure 6); and the chela manus, and fingers are uniformly yellowish-brown (Figures 7 and 8); denticles black.

Mesosoma. Brown in male; the sternum, genital operculum, basal plate, and coxae are yellowish-brown; poststernites III–VII are brown with yellow margin (Figures 3 and 5). The pectines are uniformly pale cream in color (Figures 3B).

Metasoma. It appears yellowish-brown dorsally; yellowish-brown with light brown reticulations both laterally and ventrally; feature reddish brown carinae.

Telson. The vesicle is yellowish-brown, while the aculeus is reddish-brown basally, reddish-black at tip (Figures 9).

Legs. All segments are uniformly yellow, without any spots in adult male (Figure 10).

3.8. Carapace and mesosoma:

Carapace. The carapace of *A. nazarii* sp. nov. is trapezoidal, slightly longer than wide, with an almost straight anterior margin furnished with several stout macrosetae. In the adult male holotype, it measures 7.8 mm in length, with a length-to-posterior-width ratio of 1.02 and a length-to-anterior-width ratio of 1.74 (Table 1). The surface is dominated by multiple prominent carinae adorned with medium-sized, rounded granules. The intercarinal surfaces are densely covered with small granules, except for the predominantly smooth regions between the posterior median carinae and between and around the median eyes, which bear only finely scattered granules. The anterior region of the carapace features medium-sized, flattened granules. The median ocular tubercle is situated slightly anterior to the carapace center. The ratio of the distance from the median eye center to the anterior carapace margin versus the total carapace length is 0.40; the ratio to the posterior margin is 0.56. The median eyes are positioned on either side of the anterior median carinae and are separated by a distance of nearly two ocular diameters (Figures 3 and 5). Five pairs of small, aligned lateral eyes are present, located above an area of finely granulated cuticle (Figure 5).

Sternopectinal area. The sternum is pentagonal, longer than wide, and smooth. The genital operculum is longitudinally divided; in males, the two lateral plates are typically partially separated (Figures 3B). The pectines are long, densely setose, and extend beyond the coxatrochanter joint of leg IV. The pectinal tooth count in the adult male is 27–28, with each comb possessing 3 marginal and 7 median lamellae.

Tergites. The tergites are densely granular. Tergites I-VI are tricarinate, with three moderate to strong carinae that project beyond the posterior margin. Their posterior margins also feature a distinct row of large, robust granules. The pretergites are finely granular, while the posttergites are more coarsely granular and moderately covered with rounded, moderate-sized granules, except between the lateral carinae where the fine granulation is denser. In contrast, tergite VII is smooth and pentacarinate. Its median carinae extend only halfway across the segment. All tergital carinae bear relatively large, rounded granules (Figures 3A and 4A).

Sternites. Sternites III–VI are smooth, lack granules and carinae, and each bears a pair of vestigial furrows and ventral spiracles (Figures 3B and 4B). Notably, the superior portion of the sixth sternite's spiracle has distinct granulation. Sternite VII differs markedly, exhibiting two pairs of strong granular carinae while maintaining a smooth intercarinal surface.

Pedipalp: The pedipalps robust, of moderate length, and densely setose.

Archives of Razi Institute Journal

Table 1. Morphometric comparison of adult and immature males of *A. nazarii*

Character	Species	
	♂-HT	♂-PT
CL	7.80	4.96
CPW	7.63	4.71
CAW	4.47	3.52
CL/CPW	1.02	1.05
CL/CAW	1.74	1.41
CHL	13.01	9.99
ML	5.35	3.64
MFL	7.14	6.49
Mt(I)L/W/D	5.16/5.35/4.81	3.27/3.55/3.03
Mt(II)L/W/D	6.19/5.57/4.88	4.11/3.89/3.27
Mt(III)L/W/D	6.76/5.83/5.1	4.17/3.94/3.42
Mt(IV)L/W/D	7.66/5.68/5.25	5.14/3.90/3.56
Mt(V)L/W/D	7.77/4.88/3.86	5.22/3.33/2.73
Mt(I)L/W	0.96	0.92
Mt(I)L/D	1.07	1.07
Mt(II)L/W	1.11	1.06
Mt(IV)L/D	1.46	1.44
Mt(V)L/D	2.01	1.91
TelsonL/W/H	7.02/2.87/2.23	4.59/1.91/1.7
TL/W	2.45	2.40
TL/D	3.15	2.7
No.PT	27-28	26-27
No.FFT	15	14
No.MFT	16	15
Met L	33.85	23.94
Total body L	66.88	44.58

Femur. The femur is moderately slender and pentacarinate, with all five carinae well-developed and bearing moderate granulation (Figure 6). The dorsal prolateral (dorsointernal), dorsal retrolateral (dorsoexternal), and ventral median carinae are strong and adorned with moderate, rounded granules; the ventral prolateral (ventrointernal) carina features distinct, coarse, spaced, and conical granules that are larger than those on adjacent carinae; the ventral retrolateral (ventroexternal) carina is strong and bears moderate-sized, conical granules that become more spaced anteriorly. The dorsal intercarinal surface has scattered fine granules; the inner surface is covered with scattered granules of various sizes; the ventral surface bears very few granules of various sizes; the outer surface is covered anteriorly with a few irregular fine and coarse granules, has very few scattered fine granules on the posterior two-thirds, and lacks granules posteriorly (Figure 6).

Patella. The patella is moderately slender, straight, and octocarinate. The dorsal, ventral, and external surfaces are smooth and lack granules, while the internal surface

is covered with scattered fine granules. The dorsal prolateral (dorsointernal) carina is strong and strongly crenulated, bearing coarse, pointed, spaced, conical granules that decrease in size posteriorly; it is demarcated anteriorly by a large macroseta and accompanied by a well-developed dorsal patellar spur. The dorsal prolateral median carina is very strong with more developed corneation and bears distinct, moderate, rounded granules from anterior to posterior. The dorsal retrolateral median carina is moderately strong with moderate, rounded granules but is obsolete on the anterior one-fifth. The dorsal retrolateral (dorsoexternal) carina is weak, with indistinct and flattened granules, obsolete anteriorly, and curves posteriorly towards the dorsal retrolateral median carina. On the ventral side, the ventral prolateral (ventrointernal) carina is strong and granular, bearing relatively coarse and pointed, conical granules; it is demarcated anteriorly by a large macroseta and associated with a developed ventral patellar spur. The ventral prolateral median carina is very strong with more developed corneation and has regular, distinct, small, rounded granules. The ventral retrolateral median carina is moderately strong with rounded granules but is obsolete on the anterior and posterior one-fifth. The ventral retrolateral (ventroexternal) carina is smooth, lacks granules, and is obsolete anteriorly.

Chela. Stocky; the manus is smooth on the dorsal, external, and ventral surfaces, without carinae; the internal surface is finely granulose. In the adult male, the manus length is 5.35 mm, and the movable finger length to manus length ratio is 1.33. The fingers are partly curved and moderately elongated, with the movable finger being 7.14 mm long in the adult male. The dorsal surface of the movable finger possesses fine setae, while the fixed finger lacks setae, except posteriorly. Both the pedipalp fixed and movable fingers are flanked by external and internal accessory denticles. The fixed and movable fingers possess 15–16 rows of denticles, complete with external and internal accessory granules; the movable finger also has three distal granules (Figure 6).

3.8.2. Metasoma and telson

The combined length of the metasoma and telson is 50.6–57.8% of the total body length in the adult male.

Metasoma. Robust, dorsal surfaces of all segments smooth and without setose, lateral and ventral surfaces very sparsely setose. Ventral surface of segment I smooth; segments II–IV smooth but with very few scattered fine to moderate granules, increasing slightly in density on segment IV; segment V smooth dorsally and laterally, but ventrally granulate with scattered moderate and fine granules. Segment I is longer than deep and occasionally wider than long. Segments II–V are longer than wide; segments I–V wider than deep. The width increases gradually from segment I to III, then decreases gradually from segment III to V. Segment V is the longest and least wide segment, whereas segment III is the widest. Morphometric ratios for the adult male are as follows: Segment I length/width 0.96, length/depth 1.07; segment II length/width 1.11; segment IV length/depth 1.46; segment V length/width 1.59, length/depth 2.01. The dorsal furrow moderately deep and wide on all segments; metasoma exhibits a distinct pattern of serial carinal reduction: segment I has 10 carinae, comprising paired dorsal, dorsolateral, lateral inframedian, ventral median, and ventral lateral carinae; the lateral inframedian carinae are complete and moderate; segment II has 10 carinae, but the lateral inframedian are incomplete, present only on the posterior quarter as four granules. Segment III has 10 carinae, with the lateral inframedian reduced to three granules; segment IV has eight carinae (paired dorsal, dorsolateral, ventral median, and ventral lateral carinae); segment V has five carinae (paired dorsolateral and ventral lateral carinae, and a single ventral median carina). The dorsal carinae are paired on segments I–IV, strong, and bear serrate granules that are slightly enlarged posteriorly; on segments II–IV, the dorsal carinae terminate in two enlarged, acuminate granules, which achieve their maximum development on segment IV; the posterior end of the dorsal carina on segments II and III features one or two small granules spaced apart from the terminal, largest granule, while on segment IV it ends directly with the largest granule; this carina is absent on segment V. The dorsolateral carinae are paired on all segments; on segments I–IV they are strong with rounded granules, while on segment V they are strong, bearing very rounded granules anteriorly that fuse and become smooth posteriorly. The ventral median carinae are strong and of moderate development on segments I–V, bearing moderately rounded granules; they are paired on segments I–IV and single on segment V. Paired ventral lateral carinae are present on all metasomal segments, strong on segments I–IV and bearing large, rounded granules; on segment V, the carinae remain strong, with granules that gradually enlarge posteriorly and feature four terminal granules that are markedly enlarged and widely spaced (Figure 9). The lateral inframedian carinae are subject to serial reduction: fully developed and strong on segment I, they are represented by four coarse granules on segment II, only three granules on segment III, and are entirely absent from segments IV and V (Figure 9).

Telson. The telson is slender and elongate, with a setose, ridged, and granulated ventral surface and a smooth dorsal surface (Figure 9); the aculeus is robust, elongate, and moderately curved. In the adult male, the telson is 7.02 mm long, with a length/width ratio of 2.45 and a length/depth ratio of 3.15 (Figure 9).

3.8.2. Legs:

Long, slender, covered with macrosetae; the tarsus, basitarsus, and tibiae of legs I–IV are densely covered dorsally and ventrally; the femur and patella of legs I and II are also covered dorsally and ventrally. In contrast, the femur and patella of legs III and IV are covered only ventrally. The patella of these segments has only a few bristle combs, while the femur has relatively very few bristle combs dorsally (Figure 10).

3.9. Affinities

A. nazarii sp. nov. can be distinguished from all other species of the genus by the following characters: The overall coloration is brownish-yellow (Figure 3), contrasting with the dark brown of *A. zagrosensis*, *A. barahoeii*, and *A. sumericus*; the black of *A. crassicauda*; and the yellow of *A. sistanus*. The carapace is predominantly light brown and lacks black patches, especially in the ocular area, whereas it is dark brown to black with black patches in *A. zagrosensis*, *A. barahoeii*, *A. sumericus*, *A. crassicauda*, *A. orientalis*, *A. caspius*, and *A. azerianus*; it is yellow but with ocular black patches in *A. sistanus*. The carapace granulation in *A. nazarii* sp. nov. is dense and fine, lacking large anterior granules, unlike in *A. zagrosensis*, *A. crassicauda*, *A. orientalis*, *A. azerianus*, *A. barahoeii*, *A. caspius*, and *A. sumericus*, which possess large, rounded anterior granules. All segments of the legs are uniformly yellow in *A. nazarii* sp. nov. And *A. sistanus*, but brown in A. sumericus, *A. barahoeii*, and *A. zagrosensis*. The metasoma and telson are yellowish-brown in *A. nazarii* sp. nov., but reddish-brown in *A. zagrosensis*, *A. sumericus*, and *A. barahoeii*; in *A. sistanus*, the overall color is yellow, but metasomal segments IV–V and the telson are black. The chela manus is uniformly yellowish-brown in *A. nazarii* sp. nov., whereas it is uniformly reddish-brown with black lines in *A. zagrosensis* (Figure 7), darker reddish-brown with spots and reticulations in *A. crassicauda*, and uniformly brown to yellowish-brown in *A. sumericus* and *A. barahoeii*. The internal surface of the chela manus is densely covered with fine granules in *A. nazarii* sp. nov., *A. crassicauda*, *A. barahoeii*, and *A. sumericus*, but is smooth in *A. zagrosensis*. The pedipalp fingers are uniformly yellowish-brown in *A. nazarii* sp. nov., *A. zagrosensis*, *A. barahoeii*, and *A. sumericus*, but black in *A. crassicauda*. Regarding the patella, in *A. nazarii* sp. nov. the dorsal, ventral, and external surfaces are smooth and the internal surface is finely granulated; in *A. zagrosensis* all surfaces are smooth; and in *A. sumericus* and *A. barahoeii* it is granulate on the dorsal and internal surfaces but smooth externally. The intercarinal surface of tergite VII is smooth in *A. nazarii* sp. nov., but granulated in *A. barahoeii*, *A. crassicauda*, *A. orientalis*, and *A. sistanus*. The sternites III-VII are uniformly colored with dull yellow posterior margins in *A. nazarii* sp. nov. (Figures 4B and 4D), whereas sternites VI-VII are dark brown to black and lack posterior margins in *A. sumericus*, *A. barahoeii*, and *A. zagrosensis*. The sixth sternite is smooth and lacks carinae in *A. nazarii* sp. nov. (Figures 4B and 4D), *A. zagrosensis*, *A. barahoeii*, and *A. sumericus*, but is carinate and granulate in *A. orientalis* and *A. crassicauda*. The intercarinal surface of sternite VII is smooth in *A. nazarii* sp. nov. (Figures 4B and 4D), *A. zagrosensis*, *A. orientalis*, and *A. sumericus*, but has fine and abundant granules in *A. crassicauda*. For the metasoma, in *A. nazarii* sp. nov. segments I–V are smooth dorsally and laterally and granulate ventrally; in *A. zagrosensis*, segments I–IV are entirely smooth and segment V is smooth dorsally and laterally but granulate ventrally; in *A. sumericus*, segments I–V are smooth dorsally but densely granulate laterally and ventrally; and in *A. barahoeii*, segments I–V are smooth dorsally and laterally, but segments II–V are granulate ventrally.

4. Discussion

The discovery of *A. nazarii* sp. nov. from Baghmalek in Khuzestan Province is a significant contribution to the ongoing revision of the *A. crassicauda* species complex in Iran and the broader Middle East. This finding underscores the cryptic diversity within the genus *Androctonus*, a pattern that has become increasingly apparent through recent integrative taxonomic studies [15, 17, 20, 22]. For years, populations in southwestern Iran were inconsistently reported under the name *A. crassicauda* [1, 14], obscuring the true species richness of the region. The present study clarifies the taxonomic identity of the Baghmalek population, confirming it as a distinct species that is morphologically separable from its congeners, particularly the recently described sympatric and parapatric species *A. zagrosensis*, *A. barahoeii*, and *A. sumericus*.

The distinct morphological identity of *A. nazarii* sp. nov. is established by a suite of diagnostic characters, most notably its unique coloration and granulation patterns. The overall brownish-yellow coloration provides an immediate and stark contrast to the dark brown of *A. zagrosensis*, *A. barahoeii*, and *A. sumericus*, the black of *A. crassicauda*, and the uniform yellow of *A. sistanus*. Critically, the carapace of *A. nazarii* sp. nov. lacks the

large, rounded anterior granules that are characteristic of nearly all its regional congeners, including *A. zagrosensis*, *A. barahoeii*, *A. sumericus*, and *A. crassicauda*. Instead, it exhibits dense, fine granulation. This character alone is a powerful diagnostic tool. Furthermore, the absence of black patches in the ocular area distinguishes it from species like *A. sistanus*, which, despite having a yellow carapace, retains these distinctive patches.

The unique identity of *A. nazarii* sp. nov. is further solidified by distinct morphological characteristics of its pedipalps and metasoma. Its chela manus is uniformly yellowish-brown, distinguishing it from the marked manus of relatives like *A. zagrosensis* and *A. crassicauda*. Furthermore, a unique combination of granulation patterns—specifically, a smooth intercarinal surface on both tergite VII and sternite VII, coupled with metasomal segments that are smooth dorsally and laterally but granulate ventrally, creates a morphological profile not found in any compared species. The description of *A. nazarii* sp. nov. from Baghmalek adds another piece to the complex biogeographic puzzle of the Zagros Mountains and the Khuzestan Plain. The fact that multiple morphologically distinct *Androctonus* species (*A. nazarii* sp. nov., *A. zagrosensis*, *A. barahoeii*) have been identified in relatively close proximity within the Zagros range suggests that this region has acted as a cradle for allopatric speciation, potentially driven by microhabitat specialization or historical vicariance events. The sympatric report of *A. sumericus* and *A. barahoeii* in other parts of Khuzestan [15, 20] further highlights the province as a significant biodiversity hotspot for scorpions, requiring careful species-level identification for accurate distribution records.

5. Conclusion

In conclusion, the identification of *A. nazarii* sp. nov. reaffirms that the taxonomic resolution of the *A. crassicauda* complex is far from complete. It demonstrates that even within a well-studied country like Iran, and in a genus of significant medical concern, new species await discovery in regions with complex topography. Future research should employ molecular phylogenetics to corroborate the morphological species boundaries proposed here and to elucidate the evolutionary relationships within this rapidly diversifying species group. Such integrative approaches will be essential for a comprehensive understanding of *Androctonus* diversity, biogeography, and its implications for human health.

Acknowledgements

The authors sincerely thank Sina Taghavi Moghadam for his valuable collaboration in this research. We also wish to posthumously honor and dedicate this work to the memory of the late Ahmad Taghavi Moghadam. Furthermore, we are grateful to the Razi Vaccine and Serum Research Institute, Agricultural Research, Education and Extension Organization (AREEO), in Karaj, Iran, for their support with laboratory equipment and facilities.

Compliance with ethical guidelines

All sample collection methods and experimental procedures described herein were rigorously reviewed and approved by the Institutional Animal Care Committee of Razi Vaccine and Serum Research Institute, Karaj, Iran (Code: IR.RVSRI.REC.1401.017) and AREEO protocols, which comply with Iran guidelines for work with animals.

Data availability

The data that support the findings of this study are available on request from the corresponding author.

Funding

Research conducted at Razi Vaccine and Serum Research Institute without external funding.

Authors' contributions

Conceptualization, study design, and writing the original draft: Fatemeh Salabi and Seyed Mahdi Kazemi; Data collection: All authors; Data analysis and interpretation: Fatemeh Salabi. Photography: Bahman Zangi; Review and editing: Fatemeh Salabi, Mohammad Hossein Jahan-Mahin, and Seyed Mahdi Kazemi.

Conflict of interest

The authors declared no conflict of interest.

References

[1] Salabi F, Jafari H, Mahdavinia M, Azadnasab R, Shariati S, Baghal ML, et al. First transcriptome analysis of the venom glands of the scorpion Hottentotta zagrosensis (Scorpions: Buthidae) with focus on venom lipolysis activating peptides. Frontiers in Pharmacology. 2024; 15:1464648. [DOI:10.3389/fphar.2024.1464648] [PMID]

[2] Salabi F, Vazirianzadeh B, Baradaran M. Identification, classification, and characterization of alpha and beta subunits of LVP1 protein from the venom gland of four Iranian scorpion species. Sci Rep. 2023; 13(1):22277. [DOI:10.1038/s41598-023-49556-6] [PMID]

[3] Salabi F, Jafari H. Whole transcriptome sequencing reveals the activity of the PLA2 family members in Androctonus crassicauda (Scorpionida: Buthidae) venom gland. FASEB J. 2024; 38(10):e23658. [DOI:10.1096/fj.202400178RR] [PMID]

[4] Salabi F, Jafari H. Dataset of PLA2 family identified from transcriptomic high-throughput sequencing of Androctonus crassicauda (Scorpionida: Buthidae) venom gland. Data Brief. 2024; 55:110629. [DOI:10.1016/j.dib.2024.110629] [PMID]

[5] Olson DM, Dinerstein E, Wikramanayake ED, Burgess ND, Powell GV, Underwood EC, et al. Terrestrial Ecoregions of the World: A New Map of Life on Earth: A new global map of terrestrial ecoregions provides an innovative tool for conserving biodiversity. BioScience. 2001; 51(11):933-8. [DOI:10.1641/0006-3568(2001)051[0933:TEOTWA]2.0.CO;2]

[6] Safaei-Mahroo B, Ghaffari H, Fahimi H, Broomand S, Yazdanian M, NajafiMajd E, et al. The herpetofauna of Iran: Checklist of taxonomy, distribution and conservation status. Asian Herpetol Res. 2015; 6(4):257-90. [Link]

[7] Kazemi SM, Hosseinzadeh MS, Weinstein SA. Identifying the geographic distribution pattern of venomous snakes and regions of high snakebite risk in Iran. Toxicon. 2023; 231:107197. [DOI:10.1016/j.toxicon.2023.107197] [PMID]

[8] Kazemi SM, Sabatier JM. Venoms of Iranian Scorpions (Arachnida, Scorpiones) and Their Potential for Drug Discovery. Molecules. 2019; 24(14):2670. [DOI:10.3390/molecules24142670] [PMID]

[9] Baradaran M, Salabi F, Mahdavinia M, Mohammadi E, Vazirianzadeh B, Avella I, et al. ScorpDb: A Novel Open-Access Database for Integrative Scorpion Toxinology. Toxins. 2024; 16(11):497. [DOI:10.3390/toxins16110497] [PMID]

[10] Kazemi SM, Lari Baghal M, Salabi F. Androctonus zagrosensis sp. nov., a new medically important scorpion species from Khuzestan Province, Iran (Scorpiones: Buthidae). J Nat Hist. Forthcoming. 2025.

[11] Prendini L. Phylogeny of Parabuthus (Scorpiones, Buthidae). Zool Scr. 2001; 30(1):13-35. [DOI:10.1046/j.1463-6409.2001.00056.x]

[12] Lourenço WR, Qi JX. A new species of Androctonus Ehrenberg, 1828 from Afghanistan (Scorpiones, Buthidae). Zool Middle East. 2006; 38(1):93-7. [DOI:10.1080/09397140.2006.10638170]

[13] Olivier GA. Voyage dans l'Empire Othoman, l'Egypte et la Perse. Paris: Henri Agasse; 1807. [Link]

[14] Gharakhloo MM, Heydaraba SA, Yağmur EA. The scorpion fauna of West Azerbaijan Province in Iran (Arachnida: Scorpiones). Biharean Biol. 2018; 12(2):84-7. [Link]

[15] Yağmur EA, Kovařík F, Fet V, Lowe G, Moradi M, Kalami F. A review of Androctonus of Iran, with redescription of A. crassicauda (Olivier, 1807) and A. orientalis (Birula, 1900) stat. n., and descriptions of four new species (Scorpiones: Buthidae). Euscorpius. 2025; (422):1-69. [Link]

[16] Yağmur EA, Kachel HS, Al-Khazali AM, Al-Jubouri MAK, Ali FR. Androctonus Ishtar sp. n. from Dohuk and Nineveh provinces, Iraq (Scorpiones: Buthidae). J Nat Hist. 2025; 59(25-28):1757-73. [DOI:10.1080/00222933.2025.2496290]

[17] Lowe G. The genus Androctonus Ehrenberg, 1828 (Scorpiones: Buthidae) in Oman. Euscorpius. 2025; 2025(424):1-59. [Link]

[18] Al-Khazali AM, Yağmur EA. Androctonus sumericus sp. nov., a new scorpion from Dhi Qar Province, Iraq (Scorpiones: Buthidae). Zool Middle East. 2023; 69(4):410-9. [DOI:10.1080/09397140.2023.2284016]

[19] Alqahtani AR, Yağmur EA, Badry A. Androctonus tihamicus sp. nov. from the Mecca Province, Saudi Arabia (Scorpiones, Buthidae). ZooKeys. 2023; 1152:9-34. [DOI:10.3897/zookeys.1152.101100] [PMID]

[20] Barahoei H, Mirshamsi O, Amiri M, Moeinadini A, Rakhshani E. Integrative taxonomy reveals the existence of a new species of fat-tailed scorpions, Androctonus (Buthidae), in Iran. Turk J Zool. 2025; 49(2):48-74. [DOI:10.55730/1300-0179.3213]

[21] Birula A. Beiträge zur Kenntniss der Scorpionenfouna Ost-Persiens. Bull Acad Imp Sci St-Pétersbourg. 1900; 12(4):355-75.

[22] Salabi F. A computational study of venom as drug library: Discovery of multifunctional astacin-like metalloproteases from Androctonus zagrosensis venom gland transcriptome. Comput Biol Med. 2025; 198(Pt B):111247. [DOI:10.1016/j.compbiomed.2025.111247] [PMID]

[23] Kazemi SM, Kelisani ZG, Avella I, Lüddecke T. The need for a refined scorpion antivenom for Iran. Toxicon. 2024; 248:108033. [DOI:10.1016/j.toxicon.2024.108033] [PMID]

[24] Barahoei H, Navidpour S, Aliabadian M, Siahsarvie R, Mirshamsi O. Scorpions of Iran (Arachnida: Scorpiones): Annotated checklist, DELTA database and identification key. J Insect Biodivers Syst. 2020; 6(4):375-474. [DOI:10.52547/jibs.6.4.375]

[25] Sissom WD, Polis GA, Watt DD. Field and laboratory methods. In: Polis GA, editor. The biology of scorpions. Stanford (CA): Stanford University Press; 1990.

[26] Yağmur EA. Androctonus turkiyensis sp. n. from the Şanlıurfa province, Turkey (Scorpiones:Buthidae). Euscorpius. 2021; (341):1-18. [Link]